

# A radiation tolerant 4T pixel for space applications

Manuel Innocent

Cypress Semiconductor, Schaliënhoedreef 20B, 2800 Mechelen, Belgium.

Manuel.Innocent@cypress.com, tel +32 15 446 390, fax +32 15 448 780

Space applications require image sensors that are tolerant to the harsh radiation conditions outside the earth's atmosphere. This paper presents an image sensor pixel designed in a standard 0.18 $\mu\text{m}$  CMOS image sensor process using techniques for radiation hardening by layout. Characterization is done at different Co-60 gamma ray doses up to 1 kGy (100 krad) which is a typical requirement for space applications. No degradation of the QE, the linearity, the temporal noise or the (offset) FPN have been observed after radiation. The dark current increases with the total dose from a very low 25  $\text{e}^-/\text{s}$  at 20°C before radiation up to 750  $\text{e}^-/\text{s}$  after 0.5 kGy.

## 1. Application domain

The presented radiation tolerant 4T pixel development is the next step in the long tradition that Cypress has, through the acquisition of FillFactory, in radiation tolerant image sensor design. The pixel is designed as part of an internal Cypress project. Its primary application domain is space industry, where new sensors based on it will gradually replace Cypress current radiation tolerant 3T sensors STAR250, STAR 1000 and HAS. The specifications for this pixel are driven by the requirements for star trackers, where both low cost single chip star trackers and high-end modules will benefit from the reduced temporal noise and reduced dark current from the newly developed pixel.

## 2. Demonstrator pixels

We have currently developed radiation tolerant 10 $\mu\text{m}$  4T pixels in two different 0.18  $\mu\text{m}$  CMOS image sensor processes. One is part of a broader development test chip for space applications, including circuitry that is fully radiation hardened by layout (technology 1). The other is only a pixel which is dropped in a non-radiation tolerant test chip frame (technology 2). Both these pixels use radiation tolerant layout techniques as described in [1]. All the transistors in these pixels are circular devices. Figure 1 shows a cross section of the photo diode – transfer gate – floating diffusion combination. The photo diode n implant is buried by the photo diode p implant and separated on all sides from the STI (field oxide) by the Pwell [2]. The transfer gate is a circular device, which guarantees a low leakage current even after radiation. The floating diffusion is surrounded by the transfer gate and is as such also not touching the STI. This reduces also the floating diffusion (post-radiation) leakage current. The proposed pixel topology is very well suited for 10  $\mu\text{m}$  pixels in a 0.18 $\mu\text{m}$  technology, but does not scale well to very small pixels due to the relatively large circular transistors.

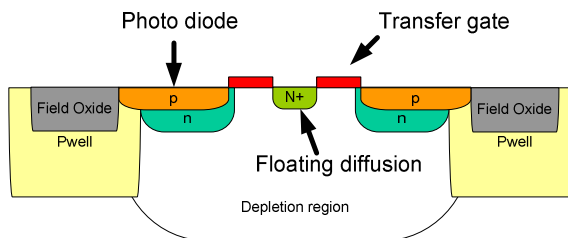


**Figure 1: Cross section of the radiation tolerant photo diode – transfer gate – floating diffusion combination. The floating diffusion is surrounded by the transfer gate, which is surrounded by the pinned photo diode.**

The two 0.18  $\mu\text{m}$  CMOS image sensor processes that are used are standard image sensor processes that are not specifically optimized for improved radiation tolerance. However, in one of the processes we fabricated samples with different implant conditions for the photo diode, which resulted in a spread of more than an order of magnitude on the post-radiation dark current after 1kGy. This data suggests that also for the other technology there is still room for further optimization.

## 3. Characterization

The 4T test chip in technology 1 has been fully characterized before radiation. Table 1 shows the key specifications of this sensor. The conversion gain is relatively low to accommodate the large saturation charge. If preferred, the conversion gain can easily be doubled without changing the topology of the pixel.

Technology	0.18 $\mu\text{m}$ CMOS image sensor process
Array size	234x234
Supply voltage	3.3V
Pixel type	4T pinned diode
Shutter type	Rolling shutter
Pixel size	10 $\mu\text{m}$ x 10 $\mu\text{m}$
QE	47% at 600nm
Conversion gain	8 $\mu\text{V}/\text{e}^-$
Pixel saturation charge	200ke $^-$
Output swing	1.6V
Temporal dark noise	0.4 mV (limited by on-chip circuits)
FPN (single ended)	9mV
FPN (CDS)	0.3mV
PRNU	0.75 % @ half saturation
Dark current (pre-radiation)	0.2mV/s at 25°C (25e $^-$ /s) 53mV/s at 70°C (6600e $^-$ /s)

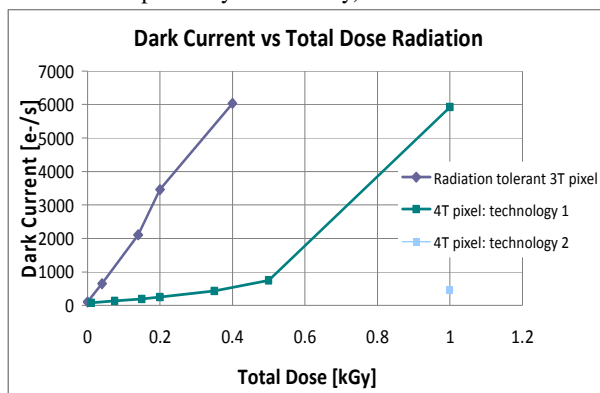
**Table 1: key specifications and measurements of the test chip in technology 1.**

The impact of radiation on CMOS circuits is typically divided into three categories: transient effects, total ionizing dose (TID) damage and displacement damage. Transient effects include circuits losing their state and radiation induced latch-up. These effects can be reduced or overcome by proper design precautions and are not part of the current study. TID damage is typically characterized by gamma ray irradiation while displacement damage is typically characterized with high energetic protons [2,3,4]. The next two sections discuss the gamma ray radiation and the proton radiation results.

#### 4. Gamma ray radiation

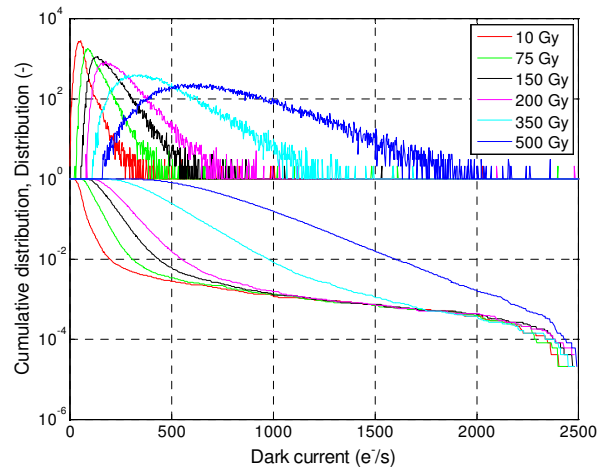
The test vehicle for the pixel characterization (in technology 1) is test chip with radiation tolerant periphery circuits and extended analogue test functionality. After 1kGy, the power consumption of the chip is unchanged within the measurement accuracy. On the samples (in technology 2) with non radiation tolerant circuits, the power consumption increased by roughly 10% after 1 kGy. Neither of the test vehicles is immune against transient effect (e.g. no triple redundant registers), so their operation may be disturbed during radiation. The gamma ray radiation on the samples of technology 1 is done with the sensors in normal operating mode. The samples in technology 2 are radiated with all their pins shorted, due to the lack of a radiation tolerant test system for this sensor. Total ionizing dose radiation testing is done using the Cobalt-60 gamma ray source at the ESTEC facility of ESA in The Netherlands.

Figure 2 shows the average dark current as a function total dose for the 4T pixels in the two different technologies and a reference 3T pixel. Compared to the radiation tolerant 3T pixel, the dark current of the pixel in technology 1 is reduced by an order of magnitude. The best process condition in technology 2 reduced the dark current by another order of magnitude (5917 e<sup>-</sup>/s versus 460 e<sup>-</sup>/s respectively after 1 kGy).



**Figure 2: Average dark current as a function total dose for 3 different sensors. The radiation tolerant 3T reference pixel is the Cypress HAS sensor, which is a state of the art radiation tolerant 3T pixel. The 4T pixels are both part of the development reported in this paper. Technology 1 is fully characterized, while for technology 2 we have only a measurement point at 1kGy, which shows an order of magnitude lower dark current than technology 1 at the same dose.**

Figure 3 shows the post-radiation dark current distribution and cumulative dark current distribution. The shape of the distribution stays very clean up to 500 Gy. The pre-radiation dark current measurement as a function of temperature shows a dark current doubling temperature of 6.0°C which indicates that the dark current is dominated by diffusion current. After 1 kGy, the doubling temperature increases to 8.4°C which indicates the generation component of the dark current has gained importance. Figure 4 shows the responsivity as a function wavelength for different radiation doses. Within the measurement accuracy, the responsivity has not been affected by the radiation. We did not observe any random telegraph signal (RTS) noise either after 1 kGy of gamma ray radiation [5]. After the radiation campaign and the post radiation characterization, the sensors of technology 1 were annealed for 168 hours (1 week) at 125°C. This anneal reduced the dark current by roughly 5x and also decreased the associated doubling temperatures.



**Figure 3 Post radiation dark current distribution (top) and cumulative dark current distribution (bottom) for different doses of gamma ray from a Co-60 source. Measurements at 25°C.**

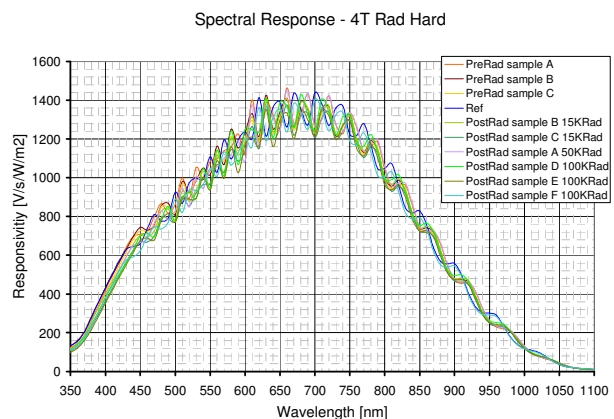


**Figure 4: Responsivity as a function wavelength pre- and post-radiation for 7 samples of the 4T test chip radiated at doses up to 1kGy gamma rays from a Co-60 source. Within the measurement accuracy, the responsivity has not been affected by the radiation.**

## 5. Proton radiation

The test vehicle for the proton radiation test is the same as for the gamma ray radiation. The proton radiation has been performed on unbiased samples (open circuit). The proton radiation tests were performed at the cyclotron research center of the university of Louvain-la-Neuve, Belgium.

Radiation is done up to a total proton fluence of  $2.4 \cdot 10^{11}$  protons /  $\text{cm}^2$  and for two proton energies: 10 MeV and 60 MeV. These are typical conditions for the characterization of displacement damage. The displacement damage caused by 10 MeV protons is larger than the damage caused by 60 MeV protons, since their non ionizing energy loss (NIEL) [6] in the silicon is about 2.4x higher ( $9.43 \text{ keV}\cdot\text{cm}^2/\text{g}$  versus  $3.37 \text{ keV}\cdot\text{cm}^2/\text{g}$ ). NIEL is a quantity that describes the rate of energy loss due to atomic displacements as a particle traverses a material. The product of the NIEL and the particle fluence (time-integrated flux) gives the displacement damage energy deposition per unit mass of material.

Both tested samples are from technology 1. Sample 1 has been radiated with 10 MeV protons and its dark current has been measured at intermediate proton fluences at the radiation site. Sample 2 has been radiated with 60 MeV protons. Both samples are characterized before and after radiation over the  $10^\circ\text{C}$  to  $60^\circ\text{C}$  range, which allows extracting the dark current doubling temperature. The dark current increases linearly with the proton fluence and the difference between the post radiation dark currents of samples 1 and 2 corresponds to the expected difference based on the NIEL difference.

As the dark current at room temperature increases due to the radiation, the dark current doubling temperature increases from  $6.0^\circ\text{C}$  to  $10.5^\circ\text{C}$ , which means the dark current increases slower with increasing temperature. This indicates the generation component of the dark current has gained importance over the diffusion component. After the radiation campaign and the post radiation characterization, both sensors were annealed for 168 hours (1 week) at  $125^\circ\text{C}$ . Similarly as after gamma ray radiation, this anneal reduced the dark current by roughly 5x on both samples and also decreased the associated doubling temperatures. The dark current increase caused by proton radiation and its annealing is similar to what is observed in our reference 3T pixel.

Table 2 summarizes the measurement results from the proton radiation campaign. Figure 5 shows the dark current distribution and cumulative dark current distribution after different proton fluences from a 10 MeV proton source. Figure 6 shows the responsivity as a function of wavelength before and after a total proton fluence of  $2.4 \cdot 10^{11}$  protons /  $\text{cm}^2$  for both 10 MeV and 60 MeV protons. Within the measurement accuracy, the responsivity has not been affected by the radiation.

Dark current ( $\text{e}^-/\text{s}$ )	Sample 1	Sample 2
(dark current doubling temperature $^\circ\text{C}$ )		
Proton energy	10 MeV	60 MeV
Pre radiation ( $25^\circ\text{C}$ )	25 ( $6.0^\circ\text{C}$ )	25 ( $6.0^\circ\text{C}$ )
Radiation (room temp)		
$0 \text{ p}^+/\text{cm}^2$ (0s)	25	
$24 \cdot 10^9 \text{ p}^+/\text{cm}^2$ (60s)	725	
$72 \cdot 10^9 \text{ p}^+/\text{cm}^2$ (180s)	4125	
$240 \cdot 10^9 \text{ p}^+/\text{cm}^2$ (600s)	15875	
Post radiation ( $25^\circ\text{C}$ )	15625 ( $10.5^\circ\text{C}$ )	6625 ( $9.6^\circ\text{C}$ )
Post high temperature anneal ( $25^\circ\text{C}$ )	3250 ( $8.2^\circ\text{C}$ )	1062 ( $7.3^\circ\text{C}$ )

**Table 2: Average dark current and dark current doubling temperature of proton irradiated sensors. The used proton flux is  $4 \cdot 10^8 \text{ p}^+/\text{cm}^2$  with energies of 10 MeV and 60 MeV respectively. Post radiation, the sensors are annealed at  $125^\circ\text{C}$  for 168 hours (7 days).**

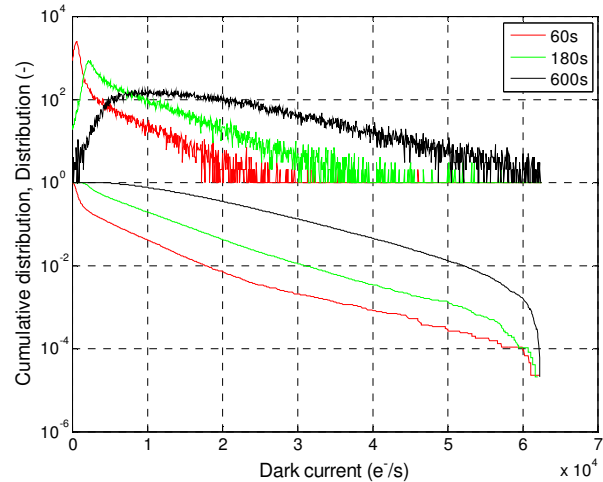


**Figure 5 Post radiation dark current distribution (top) and cumulative dark current distribution (bottom) for different proton fluences of a 10 MeV proton source. The used proton flux is  $4 \cdot 10^8 \text{ p}^+/\text{cm}^2$ . Measurements at room temperature.**

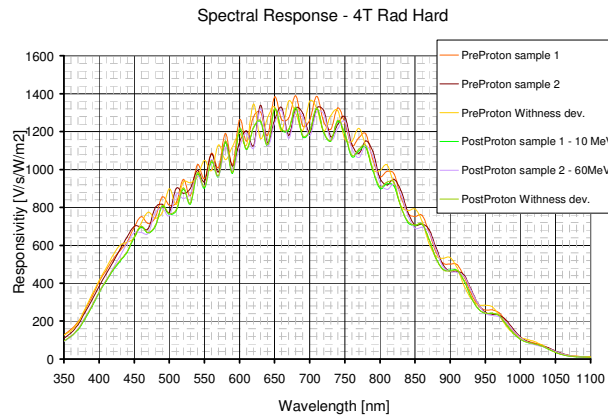


**Figure 6: Responsivity as a function wavelength pre and post-radiation for 2 samples of the 4T test chip radiated at total proton fluence of  $2.4 \cdot 10^{11}$  protons /  $\text{cm}^2$  for both 10 MeV and 60 MeV protons. Within the measurement accuracy, the responsivity has not been affected by the radiation.**

## 6. Conclusion

The presented pixel has been characterized at Co-60 gamma ray radiation levels up to 1 kGy and no degradation of the QE, the linearity, the temporal noise or the (offset) FPN have been observed after radiation. The dark current has increased but is still at a much lower level than alternative radiation tolerant 3T pixels. Similarly, the pixel has been characterized at proton fluences up to  $2.4 \cdot 10^{11}$  protons /  $\text{cm}^2$  with proton energies of 10 MeV and 60 MeV without degradation of the QE. However, the dark current increased at a similar rate than in the radiation tolerant 3T pixels. Photo diode implant variants on similar pixels in a second technology show a path for further improvement of the proposed pixel. This pixel is likely to induce a leap in star tracker performance.

## References

- [1] H. L. Hughes, and J. M. Benedetto, "Radiation Effects and Hardening of MOS Technology: Devices and Circuits," IEEE Trans. Nucl. Sci., vol. 50, pp. 500–521, Jun. 2003.
- [2] Padmakumar R. Rao, Xinyang Wang, Adri J. Mierop, and Albert J.P. Theuwissen, "Gamma-Ray Irradiation Effects on CMOS Image Sensors in Deep Sub-Micron Technology," in Proc. 2007 IEEE International Image Sensor Workshop, June 6–10, 2007, pp. 70–73.
- [3] Jan Bogaerts, Bart Dierickx, Guy Meynants, and Dirk Uwaerts, "Total Dose and Displacement Damage Effects in a Radiation-Hardened CMOS APS," IEEE Trans. Nucl. Sci., vol. 50, pp. 84–90, Jan. 2003.
- [4] J. Bogaerts, B. Dierickx, and R. Mertens, "Enhanced Dark Current Generation in Proton-Irradiated CMOS Active Pixel Sensors," IEEE Trans. Nucl. Sci., vol. 49, pp. 1513–1521, Jun. 2002.
- [5] Xinyang Wang, Padmakumar R. Rao, and Albert J.P. Theuwissen, "Characterization of the Buried Channel n-MOST Source Followers in CMOS Image Sensors," in Proc. 2007 IEEE International Image Sensor Workshop, June 6–10, 2007, pp. 223–225.
- [6] Insoo Jun, M. A. Xapsos, S. R. Messenger, E. A. Burke, R. J. Walters, G. P. Summers and T. Jordan, "Proton nonionizing energy loss (NIEL) for device applications," IEEE Trans. Nucl. Sci., vol. 50, no. 6, pp. 1924–1928, Dec. 2003.